

Supporting Information

**Core-branched CoSe₂/Ni_{0.85}Se nanotube arrays on Ni foam with remarkable
electrochemical performances for hybrid supercapacitors**

Jinghuang Lin,¹ Haohan Wang,¹ Yaotian Yan,¹ Xiaohang Zheng,¹ Henan Jia,¹ Junlei Qi*,¹ Jian Cao*,¹ Jinchun Tu*,² Weidong Fei¹ and Jicai Feng¹

1. State Key Laboratory of Advanced Welding and Joining, Harbin Institute of Technology, Harbin 150001, China

2. State Key Laboratory of Marine Resource Utilization in South China Sea, College of Materials and Chemical Engineering, Hainan University, Haikou 570228, China

*Corresponding authors: Tel. /fax: 86-451-86418146;
E-mail: jlqi@hit.edu.cn (J. L. Qi)

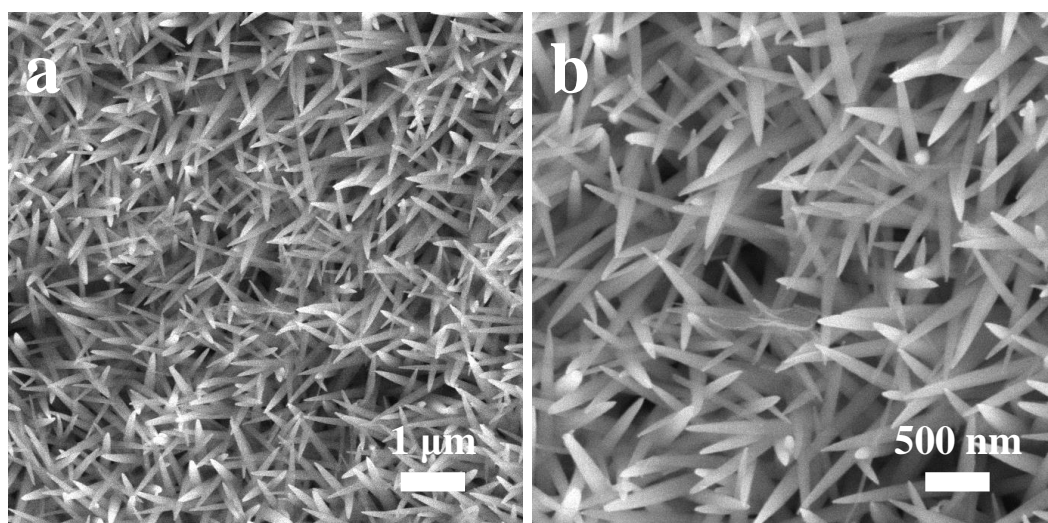


Figure S1 SEM images of Co-precursors on Ni foam.

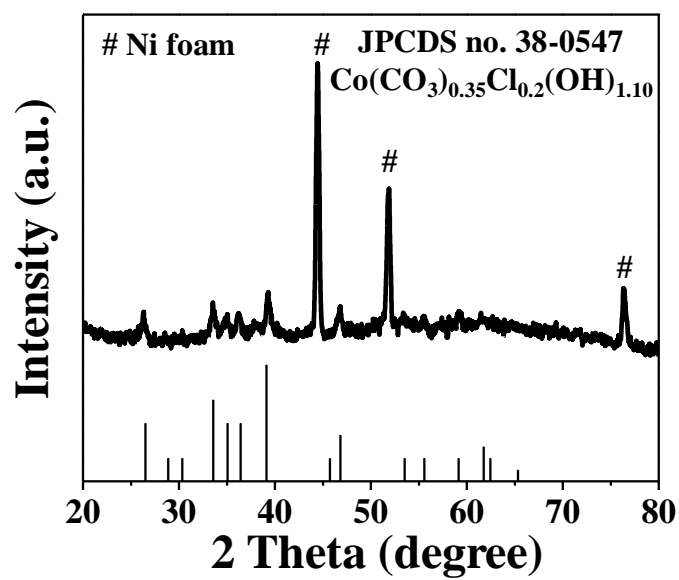


Figure S2 XRD patterns of Co-precursors on Ni foam.

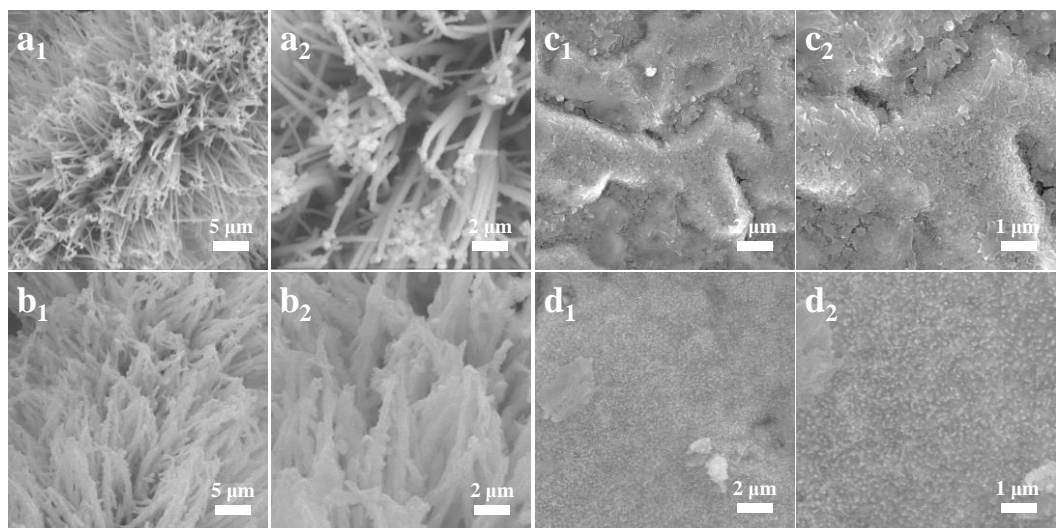


Figure S3 SEM images of (a) CoSe₂@CC, (b) E-CoSe₂@CC, (c) Ni_{0.85}Se@NF and (d) E-Ni_{0.85}Se@NF.

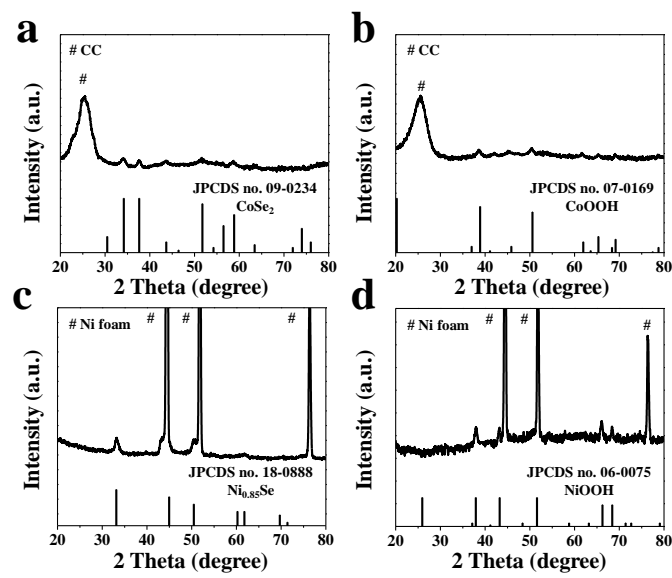


Figure S4 XRD patterns of (a) CoSe₂@CC, (b) E-CoSe₂@CC, (c) Ni_{0.85}Se@NF and (d) E-Ni_{0.85}Se@NF.

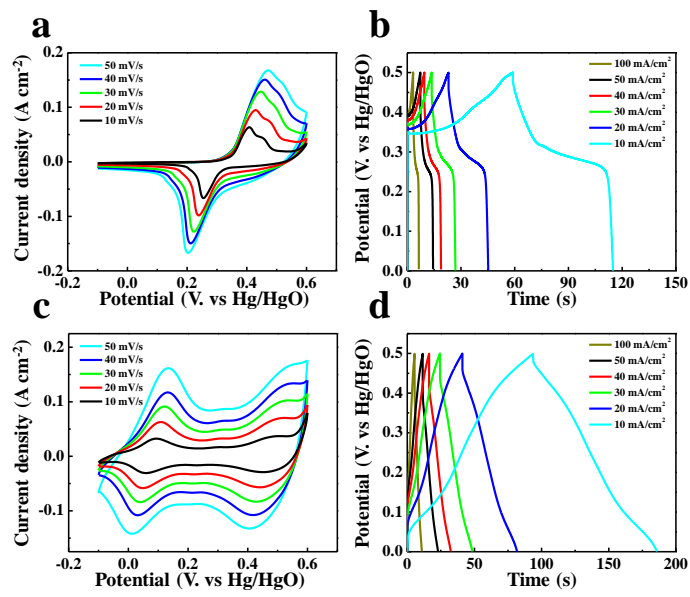


Figure S5 CV and GCD curves of (a, b) E- $\text{Ni}_{0.85}\text{Se}$ @NF and (c, d) E- CoSe_2 @CC.

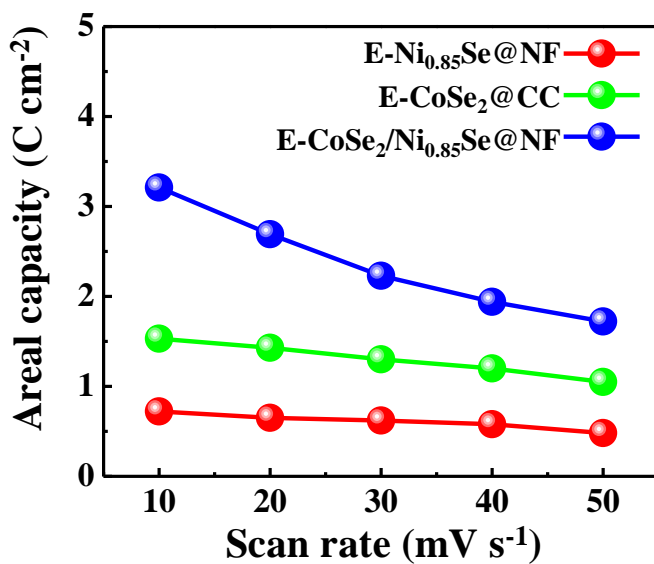


Figure S6 The calculated areal capacity of obtained electrodes via CV measurements.

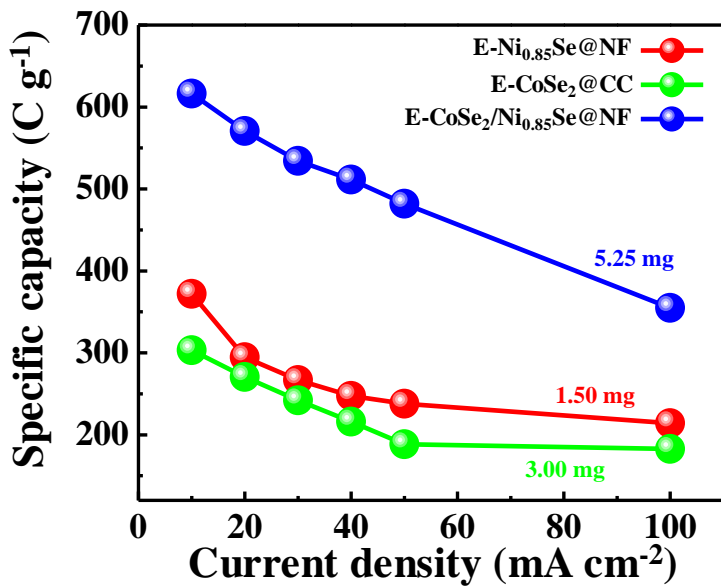


Figure S7 The calculated specific capacity of obtained samples

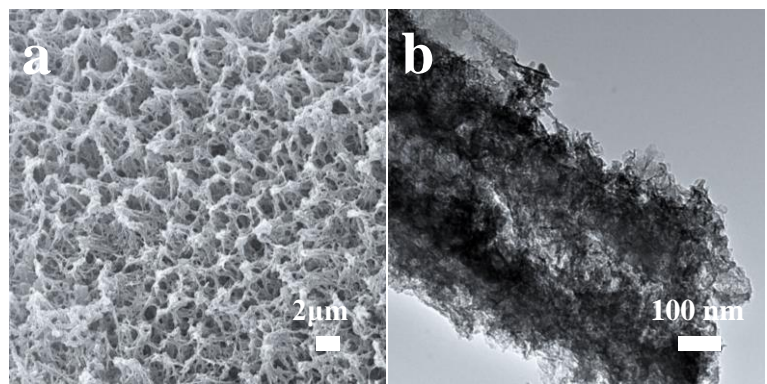


Figure S8 SEM and TEM images of E-CoSe₂/Ni_{0.85}Se@NF after cycling test.

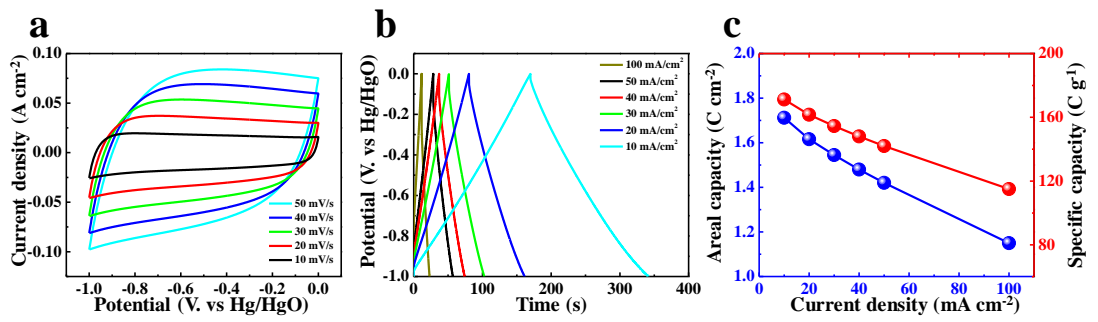


Figure S9 (a) CV, (b) GCD curves and (c) corresponding calculated capacity of AC.

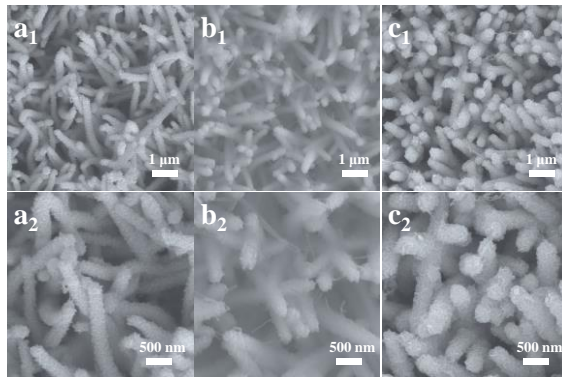


Figure S10 SEM images of (a) CoSe₂/Ni_{0.85}Se-4, (b) CoSe₂/Ni_{0.85}Se-8 and (c) CoSe₂/Ni_{0.85}Se-12.

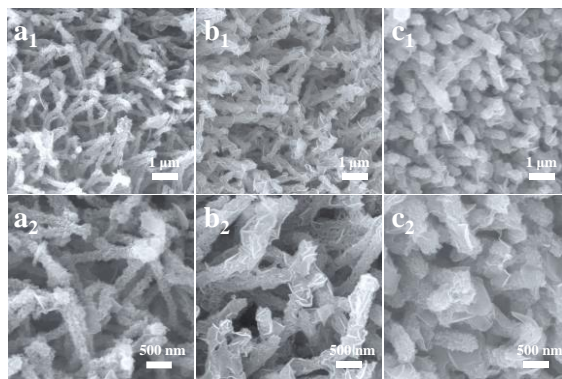


Figure 11 SEM images of (a) E-CoSe₂/Ni_{0.85}Se-4, (b) E-CoSe₂/Ni_{0.85}Se-8 and (c) E-CoSe₂/Ni_{0.85}Se-12.

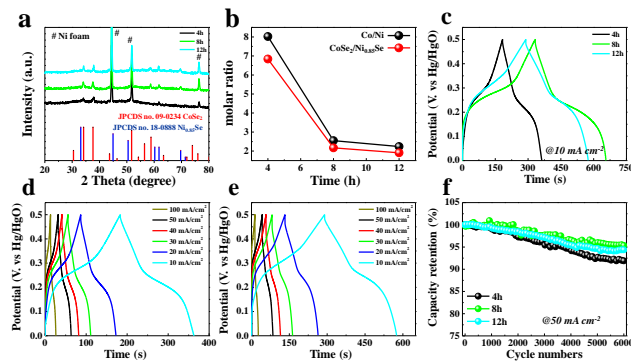


Figure 12 (a) XRD patterns of CoSe₂/Ni_{0.85}Se-4, CoSe₂/Ni_{0.85}Se-8 and CoSe₂/Ni_{0.85}Se-12. (b) The Co/Ni molar ratio and the molar ratio of CoSe₂ and Ni_{0.85}Se in obtained samples based on ICP-OES analysis. (c) GCD curves of E-CoSe₂/Ni_{0.85}Se-4, E-CoSe₂/Ni_{0.85}Se-8 and E-CoSe₂/Ni_{0.85}Se-12 at the 10 mA cm⁻² rate. (d), (e) Cyclic voltammograms at various current densities (100, 50, 40, 20, 10 mA cm⁻²). (f) Capacity retention (%) vs Cycle numbers (0 to 6000) at the 50 mA cm⁻² rate.

current density of 10 mA cm^{-2} . GCD curves of (d) E-CoSe₂/Ni_{0.85}Se-4 and (e)

E-CoSe₂/Ni_{0.85}Se-12. (f) The cycling performances of obtained electrodes.

We also prepared different electrodes by selenizing Co-precursor/Ni foam at 120°C for different hydrothermal durations (4, 8 and 12 h). For convenience, the different electrodes were denoted as CoSe₂/Ni_{0.85}Se-4, CoSe₂/Ni_{0.85}Se-8 and CoSe₂/Ni_{0.85}Se-12.

As shown in **Figure S10**, all obtained samples show the core-branched nanostructures.

It can be found that the core-branched nanotubes are becoming thicker and wider when the hydrothermal time increases from 4 h to 12 h. After electrochemical activation, the core-branched nanostructures in E-CoSe₂/Ni_{0.85}Se@NF are still maintained while more small nanosheets are formed on the surface (see **Figure S11**).

XRD pattern in **Figure S12a** confirms that all the peaks in obtained electrodes could be indexed to CoSe₂ (JPCDS no. 09-0234) and Ni_{0.85}Se (JPCDS no. 18-0888), except for the peaks from Ni substrates. The mass loadings of CoSe₂/Ni_{0.85}Se-4, CoSe₂/Ni_{0.85}Se-8 and CoSe₂/Ni_{0.85}Se-12 were estimated to about 4.13, 5.25 and 6.02 mg cm⁻². Further, we have conducted the inductively coupled plasma optical emission spectroscopy (ICP-OES) analysis to investigate the Ni/Co ratio. As shown in **Figure S12b**, the Co/Ni molar ratio of CoSe₂/Ni_{0.85}Se-4, CoSe₂/Ni_{0.85}Se-8 and CoSe₂/Ni_{0.85}Se-12 is 8.02/1, 2.55/1 and 2.24/1. Consequently, the molar ratio of CoSe₂ and Ni_{0.85}Se in CoSe₂/Ni_{0.85}Se-4, CoSe₂/Ni_{0.85}Se-8 and CoSe₂/Ni_{0.85}Se-12 are calculated to about 6.84/1, 2.17/1 and 1.91/1. In other words, the contents of CoSe₂ and Ni_{0.85}Se could be simply controlled by selenizing Co-precursor/Ni foam with different hydrothermal durations. As shown in **Figure S12c**, E-CoSe₂/Ni_{0.85}Se-8 electrode showed the longest discharge time at 10 mA cm^{-2} , indicating the highest specific capacity. And all samples also showed the good cycling stability, as shown in **Figure S12f**.

Table S1. The specific capacity of various electrodes in the three-electrode system in references

electrode materials	mass loading (mg cm ⁻²)	areal capacity	specific capacity	reference
NiSe ₂ cubes	3.9	~1.55 C cm ⁻²	~397 C g ⁻¹	1
Co _{0.85} Se on Ni foam	1	~0.76 C cm ⁻²	757.9 C g ⁻¹	2
Ni _{0.9} Co _{1.92} Se ₄ on Ni foam	6.3	~3.2 C cm ⁻²	511 C g ⁻¹	3
(Ni,Co) _{0.85} Se nanotube on CFC	-	~1.17 C cm ⁻²	-	4
Co-Cd-Se on Ni foam	2.0	~1.05 C cm ⁻²	526 C g ⁻¹	5
CoSe ₂ nanosheet on carbon cloth	0.53	~0.15 C cm ⁻²	285.3 C g ⁻¹	6
NiCoSe ₂ Hollow Sub-Microspheres	7	3.15 C cm ⁻²	450 C g ⁻¹	8
CoSe ₂ nanoarrays on carbon cloth	1.8	~0.55 C cm ⁻²	303.8 C g ⁻¹	9
Ni _{0.34} Co _{0.66} Se ₂ on carbon cloth	4.8	~1.31 C cm ⁻²	273 C g ⁻¹	10
double-shelled N-doped CoSe ₂ /C	-	-	399 C g ⁻¹	11
NiSe@MoSe ₂ on Ni foam	-	-	461.5 C g ⁻¹	12
hollow, sea-urchin-like Ni _{0.5} Co _{0.5} Se ₂	3	~1.57 C cm ⁻²	524 C g ⁻¹	13
Co _{0.85} Se@ CoNi ₂ S ₄ /GF	7	2.1 C cm ⁻²	300 C g ⁻¹	14
E-CoSe ₂ /Ni _{0.85} Se nanotube arrays	5.25	3.24 C cm ⁻²	617.1 C g ⁻¹	This work

Table S2. Comparison of the electrochemical performance of as-fabricated ASC device with those in previous reports.

Supercapattery device	Energy density (Wh kg ⁻¹)	Corresponding Power density (W kg ⁻¹)	Reference
Co _{0.85} Se//AC	39.7	789.6	2
Ni _{0.9} Co _{1.92} Se ₄ //AC	26.29	265	3
Ni _{0.85} Se@MoSe//graphene	25.5	420	7
NiCoSe ₂ //AC	25.5	3750	8
CoSe ₂ nanoarrays//carbon nanowall	32.2	1914.7	9
NiSe@MoSe ₂ //N-PMCN	32.6	415	12
Ni _{0.5} Co _{0.5} Se ₂ //RGO	37.5	745	13
Graphene wrapped Ni ₃ S ₂ /N-Graphene	32.6	399.8	15
Co ₉ S ₈ @Ni(OH) ₂ //AC	31.35	252.8	16
NiCo ₂ S ₄ @Co(OH) ₂ //AC	35.89	400	17
E-CoSe ₂ /Ni _{0.85} Se nanotube arrays//AC	40.5	538	This work

Reference

1. S. Wang, W. Li, L. Xin, M. Wu, Y. Long, H. Huang and X. Lou, *Chem. Eng. J.*, 2017, **330**, 1334-1341.
2. C. Gong, M. Huang, P. Zhou, L. Fan, J. Lin and J. Wu, *Appl. Surf. Sci.*, 2016, **362**, 469-476.
3. W. An, L. Liu, Y. Gao, Y. Liu and J. Liu, *RSC Adv.*, 2016, **6**, 75251-75257.
4. C. Xia, Q. Jiang, C. Zhao, P. M. Beaujuge and H. N. Alshareef, *Nano Energy*, 2016, **24**, 78-86.
5. Z. Zhai, K. Huang and X. Wu, *Nano Energy*, 2018, **47**, 89-95.
6. T. Chen, S. Li, J. Wen, P. Gui and G. Fang, *ACS Appl. Mater. Interfaces*, 2017, **9**, 35927-35935.
7. H. Peng, C. Wei, K. Wang, T. Meng, G. Ma, Z. Lei and X. Gong, *ACS Appl. Mater. Interfaces*, 2017, **9**, 17067–17075.
8. L. Hou, Y. Shi, C. Wu, Y. Zhang, Y. Ma, X. Sun, J. Sun, X. Zhang and C. Yuan, *Adv. Funct. Mater.*, 2018, **28**, 1705921.
9. T. Chen, S. Li, J. Wen, P. Gui, Y. Guo, C. Guan, J. Liu and G. Fang, *Small*, 2018, **14**, 1700979.
10. P. Xu, W. Zeng, S. Luo, C. Ling, J. Xiao, A. Zhou, Y. Sun and K. Liao, *Electrochim. Acta*, 2017, **241**, 41-49.
11. Y. Zhang, A. Pan, Y. Wang, X. Cao, Z. Zhou, T. Zhu, S. Liang and G. Cao, *Energy Storage Mater.*, 2017, **8**, 28-34.
12. H. Peng, J. Zhou, K. Sun, G. Ma, Z. Zhang, E. Feng and Z. Lei, *ACS Sustainable Chem. Eng.*, 2017, **5**, 5951-5963.
13. X. Song, C. Huang, Y. Qin, H. Li and H. C. Chen, *J. Mater. Chem. A*, DOI: 10.1039/c8ta05037f.

14. C. Zhang, M. Hou, X. Cai, J. Lin, X. Liu, R. Wang, L. Zhou, J. Gao, B. Li and L. Lai, *J. Mater. Chem. A*, 2018, **6**, 15630-15639.
15. J. Qi, Y. Chang, Y. Sui, Y. He, Q. Meng, F. Wei, Y. Zhao and Y. Jin, *Part. Part. Syst. Charact.*, 2017, 34, 1700196.
16. F. Zhu, M. Yan, Y. Liu, H. Shen, Y. Lei and W. Shi, *J. Mater. Chem. A*, 2017, 5, 22782-22789.
17. R. Li, S. Wang, Z. Huang, F. Lu and T. He, *J. Power Source*, 2016, **312**, 156.